Anesthesia-induced loss of consciousness disrupts auditory responses beyond primary cortex

Aaron J. Krom[a,b,c,1] , Amit Marmelshtein[d,1] , Hagar Gelbard-Sagiv[a], Ariel Tankus[d,e,f] , Hanna Hayat[a] ,
Daniel Hayat[g], Idit Matot[g], Ido Strauss[e,f], Firas Fahoum[f,h], Martin Soehle[i], Jan Boström[j], Florian Mormann[k] ,
Itzhak Fried[e,f,l,2], and Yuval Nir[a,d,2]

[a]Department of Physiology & Pharmacology, Sackler School of Medicine, Tel Aviv University, Tel Aviv 6997801, Israel; [b]Department of Anesthesiology and
Critical Care Medicine, Hadassah-Hebrew University Medical Center, Jerusalem 91120, Israel; [c]Hadassah School of Medicine, Hebrew University, Jerusalem
91120, Israel; [d]Sagol School of Neuroscience, Tel Aviv University, Tel Aviv 6997801, Israel; [e]Functional Neurosurgery Unit, Tel Aviv Sourasky Medical Center,
Tel Aviv 6423906, Israel; [f]Department of Neurology & Neurosurgery, Sackler School of Medicine, Tel Aviv University, Tel Aviv 6997801, Israel; [g]Department of
Anesthesia, Intensive Care and Pain, Tel Aviv Medical Center, Sackler Medical School, Tel Aviv University, Tel Aviv 6997801, Israel; [h]EEG and Epilepsy Unit,
Department of Neurology, Tel Aviv Sourasky Medical Center, Tel Aviv 6423906, Israel; [i]Department of Anesthesiology and Intensive Care Medicine, University of
Bonn Medical Center, 53127 Bonn, Germany; [j]Department of Neurosurgery, University of Bonn Medical Center, 53127 Bonn, Germany; [k]Department of Epileptology,
University of Bonn Medical Center, 53127 Bonn, Germany; and [l]Department of Neurosurgery, University of California, Los Angeles, CA 90095

Despite its ubiquitous use in medicine, and extensive knowledge
of its molecular and cellular effects, how anesthesia induces loss of
consciousness (LOC) and affects sensory processing remains poorly
understood. Specifically, it is unclear whether anesthesia primarily
disrupts thalamocortical relay or intercortical signaling. Here we
recorded intracranial electroencephalogram (iEEG), local field po-
tentials (LFPs), and single-unit activity in patients during wakeful-
ness and light anesthesia. Propofol infusion was gradually increased
while auditory stimuli were presented and patients responded to a
target stimulus until they became unresponsive. We found wide-
spread iEEG responses in association cortices during wakefulness,
which were attenuated and restricted to auditory regions upon
LOC. Neuronal spiking and LFP responses in primary auditory cortex
(PAC) persisted after LOC, while responses in higher-order auditory
regions were variable, with neuronal spiking largely attenuated.
Gamma power induced by word stimuli increased after LOC while
its frequency profile slowed, thus differing from local spiking activ-
ity. In summary, anesthesia-induced LOC disrupts auditory process-
ing in association cortices while relatively sparing responses in PAC,
opening new avenues for future research into mechanisms of LOC
and the design of anesthetic monitoring devices.

propofol | human | single-unit | LFP | gamma power

The practice of administering general anesthesia, which began
over 170 y ago, revolutionized medicine by transforming
surgery from being a deeply traumatic experience into a humane
therapy (1, 2) and enabling complex procedures to be performed.
In the United States, nearly 60,000 patients per day undergo
general anesthesia (3): a drug-induced, reversible condition that
includes unconsciousness, amnesia, analgesia, and akinesia. By
now, we have extensive knowledge of the molecular and cellular
effects of anesthetics (4–7), but how anesthetic drugs induce loss
of consciousness (LOC) remains a central unresolved question in
neuroscience and medicine (8). Given that anesthetics act at di-
verse molecular and cellular targets (7, 9), their effects on con-
sciousness and sensory perception are best studied at the level of
common brain circuits and systems (2, 9, 10). Indeed, recent an-
esthesia studies focusing on the systems level proposed that LOC
may involve sleep pathways (9, 11), thalamocortical circuits (12),
specific brainstem regions (2, 13, 14), or unbinding of frontopar-
ietal cortical activities (15, 16).

Traditionally, sensory pathways were studied in anesthetized
animals where robust responses in primary sensory regions promp-
ted seminal discoveries on the organizational principles in multiple
modalities (17–19). With time, research expanded to awake animals
and a number of studies directly compared sensory processing across
wakefulness and anesthesia, revealing state-dependent evoked re-
sponses in the visual (20–22) and somatosensory domains (23, 24).

However, these modalities heavily depend on active sensing (i.e., eye
movements and whisking) (25) and its absence in anesthesia limits
interpretation as reflecting LOC. In the auditory domain where
processing is largely passive, anesthesia was originally reported
to reduce responses in auditory cortex (26–28), but recent studies
with light anesthesia challenge this view (29). In humans, effects
of anesthesia have been reported for midlatency cortical evoked
potentials (30) and for high-frequency (40-Hz) steady-state poten-
tials (31). Functional magnetic resonance imaging studies revealed
differential responses across wakefulness and anesthesia (32–34),
but interpretation is limited by poor temporal resolution and by
relying on hemodynamics that change upon anesthesia (35). Gen-
erally, previous studies that compared sensory processing across
wakefulness and anesthesia mostly focused on activity up to primary
sensory cortex (26–28), often employed deep anesthesia at surgical
levels (31, 34), entailed uncertainty about the precise moment of
LOC in animal models, or relied on noninvasive measures in

Significance

We studied how anesthesia-induced loss of consciousness (LOC)
affects processing of external sensory events at single-neuron
resolution in epilepsy patients implanted with depth electrodes
for clinical treatment. Just before electrode removal, patients
were lightly anesthetized with propofol while we presented
sounds around LOC. We found that auditory responses were
widespread across the brain during wakefulness. Upon LOC,
robust responses persisted in primary auditory cortex while re-
sponses in high-order auditory regions were mostly attenuated.
In addition, gamma power responses in local field potentials
strengthened upon LOC, in contrast to spiking activities. The
disruption in sensory signaling beyond primary cortices high-
lights impaired cortical connectivity as a key factor in LOC and
may guide future development of anesthesia monitors and
anesthetic agents.

humans with limited resolution (31–34, 36). We sought to go beyond these limitations to better understand how anesthesia-induced LOC affects sensory processing. In particular, we aimed to address a central unresolved question in the field: whether anesthesia-induced LOC primarily affects bottom-up thalamocortical relay to primary sensory regions ["thalamic gating" (37, 38)] or, alternatively, whether it mainly affects cortical signaling beyond primary regions (12).

We capitalized on a unique opportunity to compare auditory responses in neurosurgical epilepsy patients implanted with depth electrodes as they were anesthetized immediately before removal of intracranial electrodes. Extending protocols successfully employed to study anesthetic LOC (39–41), we recorded intracranial field potentials and neuronal spiking activity to compare auditory responses in wakefulness and light "just-hypnotic" anesthesia, allowing us to focus on changes related to LOC. Working with human subjects capable of responding purposefully to verbal tasks allowed us to reliably assess the moment of LOC. High-fidelity auditory responses evident in individual trials enabled comparison of sensory responses in short intervals immediately before and after LOC, thereby isolating the changes most relevant to LOC and minimizing confounding effects of deep anesthesia (e.g., changes in breathing, blood circulation, and thermoregulation). Our results reveal that anesthesia-induced LOC disrupts auditory responses in association cortex, while significant early responses in primary auditory cortex are relatively preserved. This distinction was observed for both simple (click train) and complex (word) stimuli and evident in local field potentials (LFPs) as well as in single-neuron spiking activity representing neuronal output.

Results

To study the effects of anesthesia-induced LOC on sensory-evoked neuronal activity in humans, we recorded intracranial electroencephalogram (iEEG), LFPs, and neuronal spiking activity in epilepsy patients implanted with depth electrodes (Fig. 1 *A* and *B*) or subdural cortical grids/strips, as they were anesthetized immediately before removal of intracranial electrodes. In nine experimental sessions (*SI Appendix*, Table S1), individuals listened to 40-Hz click trains, and from the third session onward they were also presented with words and performed an auditory detection task. During each session the subjects were gradually anesthetized with propofol (Fig. 1 *C* and *D* and *SI Appendix*, Figs. S1 and S2).

We operationalized LOC as complete loss of behavioral responsiveness on our task. This criterion for LOC was identical throughout, allowing us to reliably identify the neural correlates associated with LOC despite inevitable variability in the anesthesia induction profiles, such as the precise propofol concentration (Fig. 1 and *SI Appendix*, Fig. S2). Although it is difficult to assess the phenomenological state once someone fails to respond and separate with certainty LOC from mere unresponsiveness (see also *Discussion*), multiple features of the anesthesia state were in line with those reported for propofol-induced LOC: 1) In the
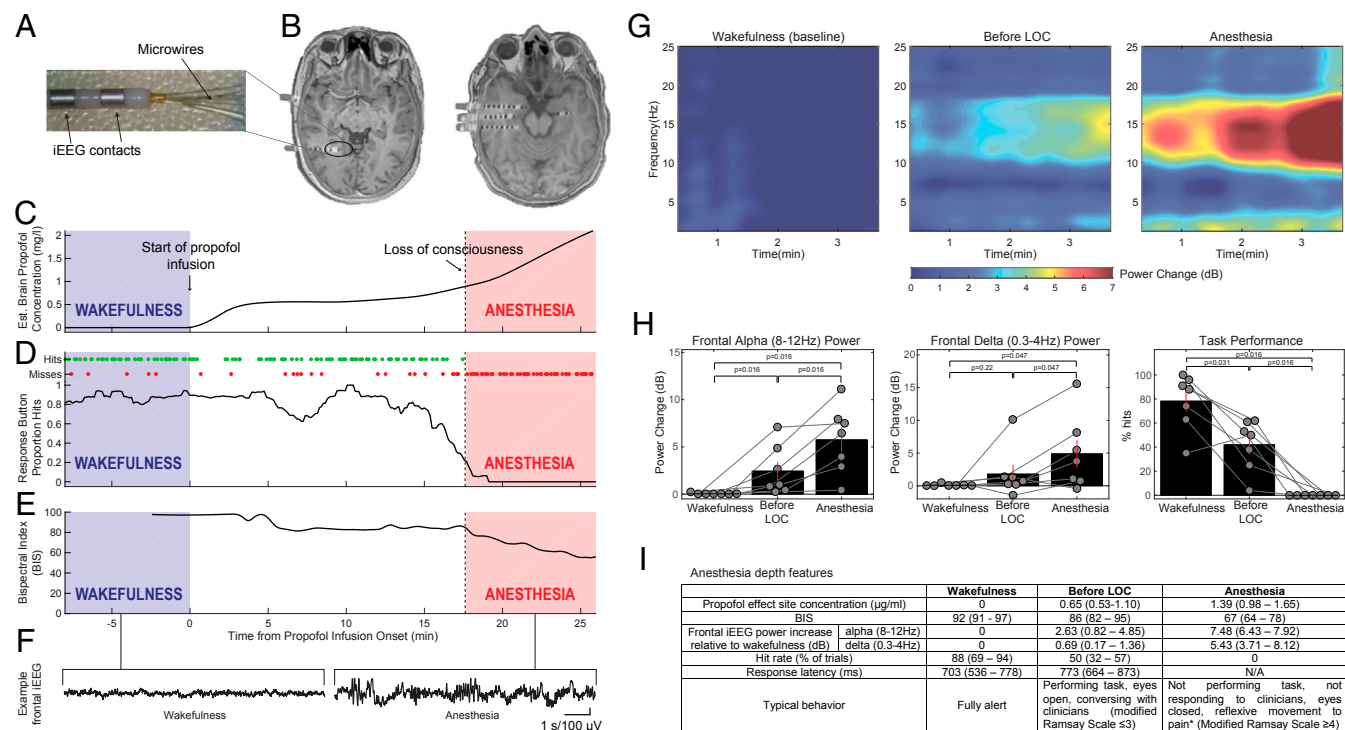

Fig. 1. Experimental setup. (*A*) Depth electrodes implanted in epilepsy patients for clinical monitoring, consisting of eight 1.5-mm iEEG contacts along the shaft and eight 40-μm microwires protruding from the distal tip. (*B*) Representative preimplant MRI coregistered with postimplant CT used to localize electrode positions in two slices from a single subject. (*C*) Representative time course of estimated propofol concentration in brain tissue (*y* axis) gradually increasing during experiment. Shaded regions mark intervals of wakefulness (blue) and anesthesia (red) used for subsequent data analysis. (*D*) Time course of behavioral performance on the auditory task (individual task hits/misses as green/red dots, plotted above averaged proportion of trials with hits). Vertical dotted line, loss of responsiveness. (*E*) Bispectral index (BIS). (*F*) Representative frontal iEEG traces during wakefulness and anesthesia. (*G*) Mean time-frequency dynamics (spectrogram) of frontal iEEG during wakefulness (*Left*), immediately before LOC (*Middle*), and anesthesia (*Right*); n = 7 sessions with frontal iEEG data. (*H*, *Left* and *Middle*) Quantification of frontal iEEG power change relative to wakefulness for alpha (8 to 12 Hz) and delta (0.3 to 4 Hz) frequency bands, respectively, showing significant increase upon LOC (n = 7). (*H*, *Right*) Behavioral task performance (percent hit rate) showing deterioration already in the minutes preceding LOC, followed by complete cessation of responses upon LOC (n = 7 sessions with behavioral task data). (*I*) Anesthesia depth measures across all sessions. Results expressed as median (interquartile range) over sessions. Response latency defined from beginning of 500-ms word. *When painful stimulus was applied at end of anesthesia period.

Krom et al.

few minutes before LOC, we already observed considerable degree of unresponsiveness typical for sedation (Fig. 1 *H* and *I*) (42); 2) frontal iEEG spectral power changes (Fig. 1 *G* and *H*) showed significant (*P* < 0.05 via Wilcoxon sign-rank test [WSRT]) increases in both alpha (8 to 12 Hz) and delta (<4 Hz) activities upon LOC, confirming that LOC was associated with additional deepening of the anesthesia state (40, 43, 44); 3) clinical rating of ongoing behavior indicated modified Ramsay scores ≥4 (45) (Fig. 1 *I*, bottom row) and responses to painful stimuli were either entirely absent or reflexive at most, suggesting LOC; and 4) median propofol effect size concentration in subjects without adjuvant agents was 0.89 μg/mL at LOC and 1.39 μg/mL during anesthesia periods (Fig. 1*I*), consistent with the reported range for propofol-induced LOC (33, 43, 46, 47). While clinically, the American Society of Anesthesiology (ASA) defines the anesthesia period we focus on here (light anesthesia co-occurring with unresponsiveness to verbal commands) as "deep sedation" (48), detailed analysis of its properties collectively strongly suggest that it reflects LOC as defined in the anesthesia research literature (33, 42–47). In each session, we compared auditory responses recorded in the first few minutes after LOC ["anesthesia," average bispectral index (49) BIS = 67, *n* = 9] with those recorded in an equally long interval during propofol-free wakefulness ("wakefulness," Fig. 1*E*, average BIS = 92).

Anesthesia-Induced LOC Disrupts Responses in Association Cortex. In wakefulness, 40-Hz click trains (Fig. 2*A*, blue ticks and *Materials and Methods*) strongly entrained field potentials such that time-locked iEEG responses were highly coherent across single trials (Fig. 2*A*). We quantified the response fidelity of each iEEG electrode (*n* = 612) by calculating its intertrial phase coherence (ITPC) (*Materials and Methods* and *SI Appendix*, Fig. S3) at 40 Hz. This measures the consistency of responses across trials on a scale of 0 (random) to 1 (perfectly consistent). During wakefulness (Fig. 2*B*), significant responses (*P* < 0.01) were found in 66% of contacts (median ITPC of all contacts = 0.40, median *P* = 4×10^{-5}, *n* = 612). Responses were observed across all cortical lobes yet exhibited spatial selectivity, with temporal contacts around auditory cortex showing the strongest responses. During anesthesia, iEEG responses in association cortices were markedly reduced (Fig. 2 *C* and *D*), with median ITPC dropping from 0.4 to 0.17, representing a 58% reduction. Accordingly, 65% of responding electrodes (*n* = 421, electrodes with responses above baseline during either wakefulness or anesthesia) showed significant reduction in ITPC (*P* < 0.05, Monte Carlo permutation test) compared to only 1.0% showing significant increase in ITPC. Robust attenuation was also evident when quantifying the distribution of gain factors between states (*Materials and Methods*), which was strongly skewed toward attenuation upon LOC (Fig. 2*E*). During anesthesia, significant (*P* < 0.01) responses persisted in only 22% of contacts (median ITPC of all contacts = 0.17, median *P* = 0.20, *n* = 612) and 95% of these responses were observed within the temporal lobe (i.e., in electrodes relatively close [26.9 ± 9.0mm] to Heschel's gyrus; temporal lobe electrodes represented 60% of all iEEG contacts). Even in iEEG contacts located closest to PAC (on the shafts targeted toward the PAC), response fidelity was markedly reduced upon anesthetic LOC (median ITPC dropped from 0.83 to 0.37, *n* = 27; 85% of such responsive electrodes significantly reduced ITPC compared to none showing significant increase). Disruption of iEEG responses in association cortices upon LOC was highly reproducible across individual sessions (*SI Appendix*, Fig. S4) and evident also when quantifying responses through event-related spectral power (ERSP, "induced power"; *SI Appendix*, Fig. S5).

Robust Responses Persist after LOC in Primary Auditory Cortex. In five sessions, microwires targeted seven regions located more medially in and around Heschel's gyrus and recorded locally
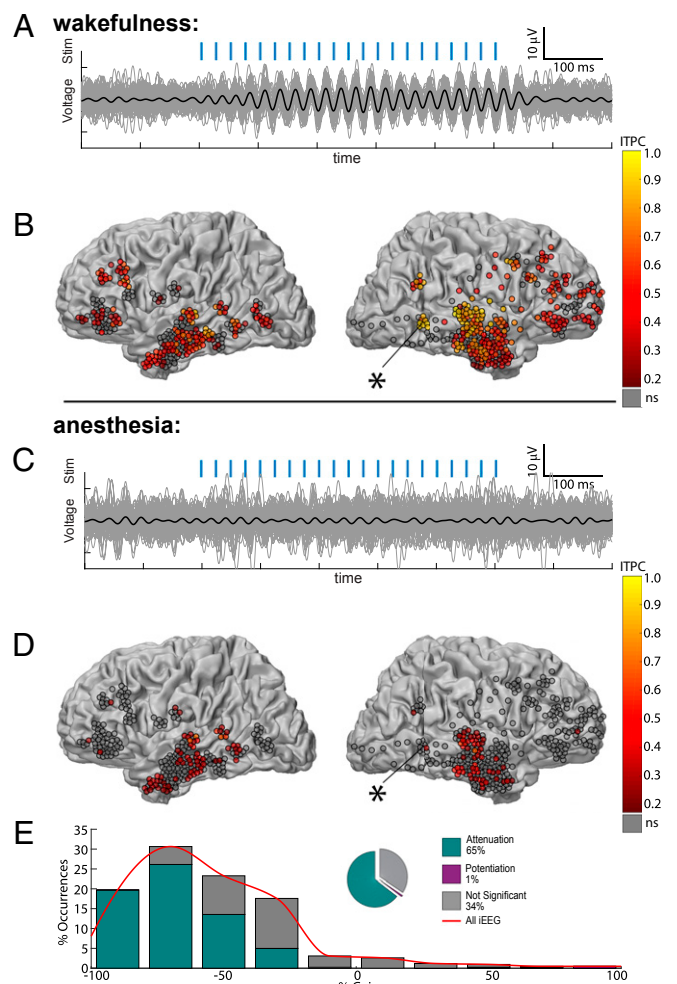

Fig. 2. Anesthesia-induced LOC disrupts auditory responses in association cortices. (*A*) Responses to 40-Hz click train (stimulus, in blue) in a representative iEEG electrode in the superior temporal sulcus (asterisk) during wakefulness. Thick black trace marks the average response, while thin gray traces show individual trials (*B*) ITPC at 40 Hz for each iEEG electrode (*n* = 612 in nine sessions) during wakefulness, as shown on a gray–white matter boundary surface as seen from lateral view. (*C*) Responses of the same iEEG electrode shown in *A* during anesthesia reveal disruption of reliable responses upon LOC. (*D*) ITPC of the same iEEG electrodes shown in *B* revealing disruption of responses outside the primary auditory cortex. (*E*) Quantification of the 421 iEEG contacts showing significant responses above baseline during either wakefulness or anesthesia, reveal that 65% undergo significant attenuation under anesthesia, compared to only 1% showing potentiation. The red curve represents the smoothed histogram and is used for comparison in later figures.

referenced LFPs (*n* = 56 microwires). Four of the seven microwire arrays (Fig. 3, pmHG1–4) were located in posteromedial Heschel's gyrus and exhibited short-latency (<30 ms) responses (*SI Appendix*, Fig. S6). For brevity, we refer to these as "primary auditory cortex" (PAC) throughout, despite the lack of systematic tonotopic mapping for delineating A1 (*Materials and Methods*). In contrast to disrupted iEEG responses in association cortices, PAC LFPs continued to show highly significant responses during anesthetic LOC (Fig. 3 *A* and *B*; median ITPC = 0.73, *n* = 32, median *P* < 10^{-15}). Accordingly, the distribution of gain factors between states was largely symmetrical and only showed modest attenuation (Fig. 3*C*), a pattern significantly different from that found in association cortices (*P* < 10^{-12} by Wilcoxon rank-sum test [WRST]), z(n_{AsC} = 421, n_{PAC} = 32) = 7.41, Cohen's d = 1.26,
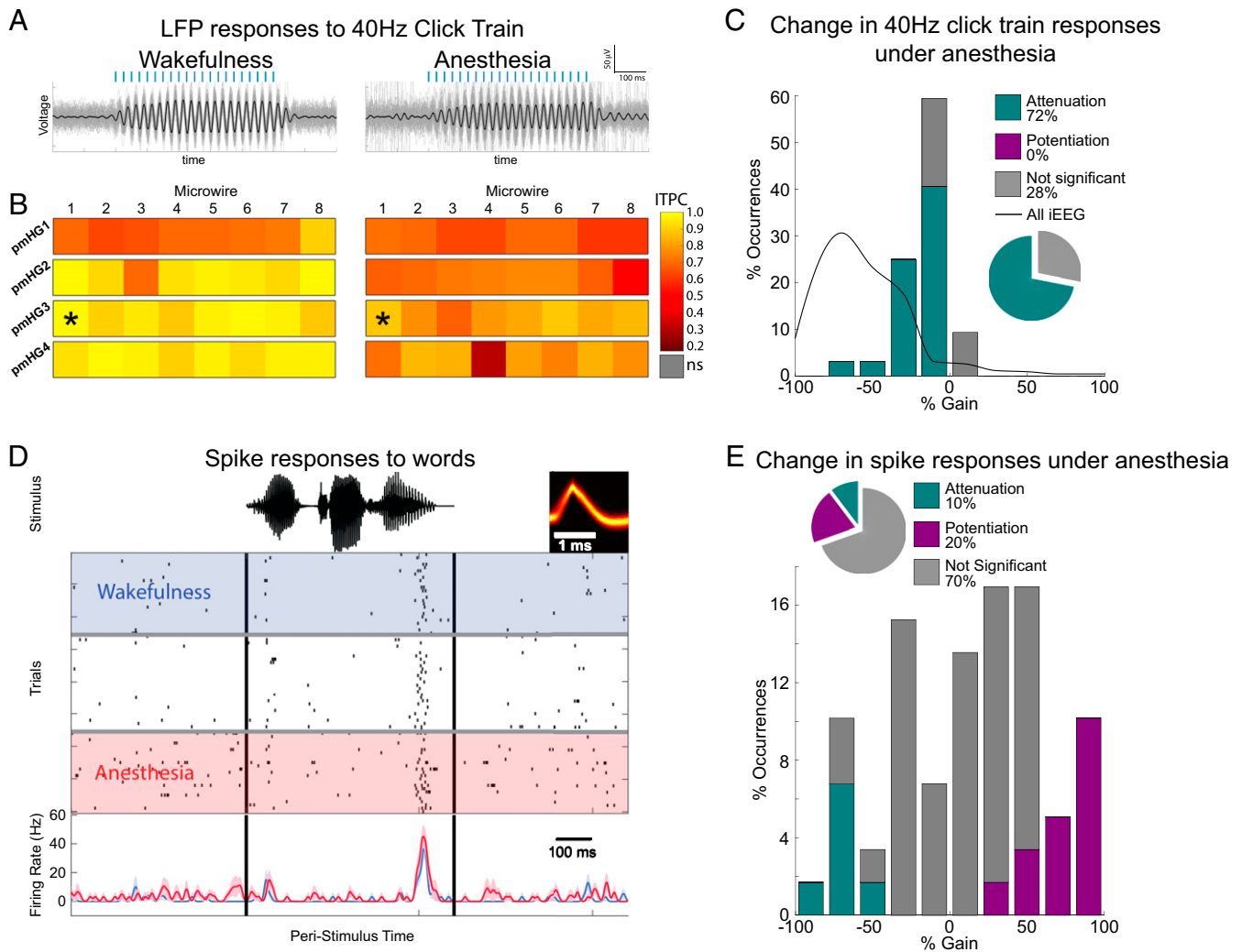
Fig. 3. Significant responses in primary auditory cortex persist upon anesthesia-induced LOC. (*A*) Band-passed responses to 40-Hz click train in a representative PAC electrode during wakefulness (*Left*) and anesthesia (*Right*). Thick black traces mark the average responses, while thin gray traces show individual trials. (*B*) Responses (ITPC) to 40-Hz click trains across all PAC microwires (*n* = 32, arrays pmHG 1–4) during wakefulness (*Left*) and anesthesia (*Right*) reveals significant responses persisting upon anesthesia-induced LOC. Asterisks mark the specific microwire whose responses are shown above. (*C*) Histogram of response gain under anesthesia for all 32 PAC microwires shows only minimal attenuation (bars), especially when compared to the marked attenuation seen across the brain in iEEG contacts (gray curve). (*D*) Raster plot and peristimulus time histogram (PSTH, below) of representative PAC neuronal response to a word (stimulus waveform on top in black; neuron spike waveform in yellow). Rows (top to bottom) mark individual trials during deepening propofol anesthesia. Blue shading and time course, wakefulness; red shading and time-course, anesthesia. (*E*) Quantitative analysis across all PAC responses (*n* = 59 in 20 neurons) reveals that 70% of responses were not significantly different between wakefulness and anesthesia, 10% were attenuated in anesthesia, and 20% were potentiated in anesthesia.

median gain −0.15 vs −0.60). Importantly, the distinction between persistent responses in PAC (median gain = −0.15, *n* = 32) and significant attenuation in adjacent iEEG electrodes (median gain = −0.47, *n* = 8) was evident when comparing these profiles in simultaneously recorded data [$P = 6 \times 10^{-3}$ by WRST, z(n_{PAC} = 32, n_{iEEG} = 8) = 2.72, Cohen's d = 1.60] as well as when comparing the average gain per PAC array with the average gain of association cortices iEEGs per session (P = 0.0028 by WRST, n_{PAC} = 4, n_{AsC} = 9, Cohen's d = 2.25, median gain −0.181 vs −0.505). In line with these ITPC results, LFP power changes in PAC microwires quantified via ERSP (*SI Appendix*, Fig. S7) showed far less attenuation than those seen in iEEG contacts across the brain [*SI Appendix*, Fig. S5; $P < 10^{-8}$ by WRST, z(n_{PAC} = 32, n_{AsC} = 190) = 5.86, Cohen's d = 1.10, median gain −0.39 vs −0.92].

Preserved PAC responses were also observed in the neuronal spiking responses to words (*n* = 59 responses in 20 units that responded in either wakefulness or anesthesia; see *SI Appendix*, Table S1 for details). Fig. 3*D* shows a representative PAC

neuron, where firing rate responses were essentially unchanged between wakefulness and anesthetic LOC (see *SI Appendix*, Fig. S8 for additional examples). A quantitative analysis across all responses (Fig. 3*E* and *Materials and Methods*) confirmed that most (70%) PAC responses did not significantly change between wakefulness and anesthetic LOC ($P > 0.05$, WRST). Only a small minority of components showed attenuation (10%), with the rest showing potentiation (20%), indicating an overall preservation of PAC spike responses. As was the case for relatively preserved LFP responses in PAC, spike responses in PAC significantly [$P < 10^{-19}$ by WRST, z($n_{unit\ responses}$ = 59, n_{AsC} = 421) = 9.2, Cohen's d = −1.99, median gain = 0.13 vs −0.60] differed from the attenuation profile observed in association cortex iEEG responses.

Higher-Order Auditory Regions Exhibit Variable Effects upon Anesthetic LOC with Spike Responses Largely Attenuated. We refer to temporal lobe regions outside PAC with higher latencies and/or weaker responses during wakefulness as higher-order auditory regions

Krom et al.

www.manaraa.com

NEUROSCIENCE

(middle Heschl's gyrus [midHG], posterior planum temporale [pPT], and anterior superior temporal gyrus [aSTG]; *SI Appendix,* Fig. S6 and *Materials and Methods*).

The midHG (response latency 52 ms [vs. 17 ms in PAC]; *SI Appendix,* Fig. S6) exhibited highly reproducible auditory responses in wakefulness (Fig. 4 *A* and *B*; median ITPC = 0.84, median $P < 10^{-21}$, $n = 8$), which dramatically attenuated to noise levels after anesthetic LOC (Fig. 4 *B* and *C, Top*; median ITPC = 0.15, median $P = 0.20$), as observed in association cortices (Fig. 4 *C, Top*). In line with LFP attenuation, neuronal spiking responses to words in this region ($n = 55$ responses in nine units responding in either wakefulness or anesthesia) strongly attenuated around LOC. Fig. 4*D* shows a representative neuronal response, demonstrating clear attenuation in firing response to a word stimulus upon anesthetic LOC (see *SI Appendix,* Fig. S8 for

additional examples). A quantitative analysis across all responses (Fig. 4*E*) showed strong response suppression, with 71% of responses significantly attenuating ($P < 0.05$, WRST), 29% showing no significant change, and none showing potentiation—a significantly different profile than the preservation of PAC unit responses [$P < 10^{-9}$ by WRST, z($n_{high-order} = 55$, $n_{PAC} = 59$) = 6.2, Cohen's d = 1.49, median gain −0.52 vs +0.13].

The pPT and aSTG showed a different response profile consisting of weak, albeit significant, auditory responses in wakefulness (Fig. 4*B*; median ITPC = 0.25, $n = 16$, median $P = 3 \times 10^{-3}$), which moderately strengthened upon anesthetic LOC (Fig. 4 *B* and *C, Bottom*; median ITPC = 0.36, median $P < 10^{-5}$). Here, 42% of microwires showed significant potentiation ($P < 0.05$, Monte Carlo permutation test), and none showed attenuation. Anecdotally, the responses of one auditory-responsive neuron identified in
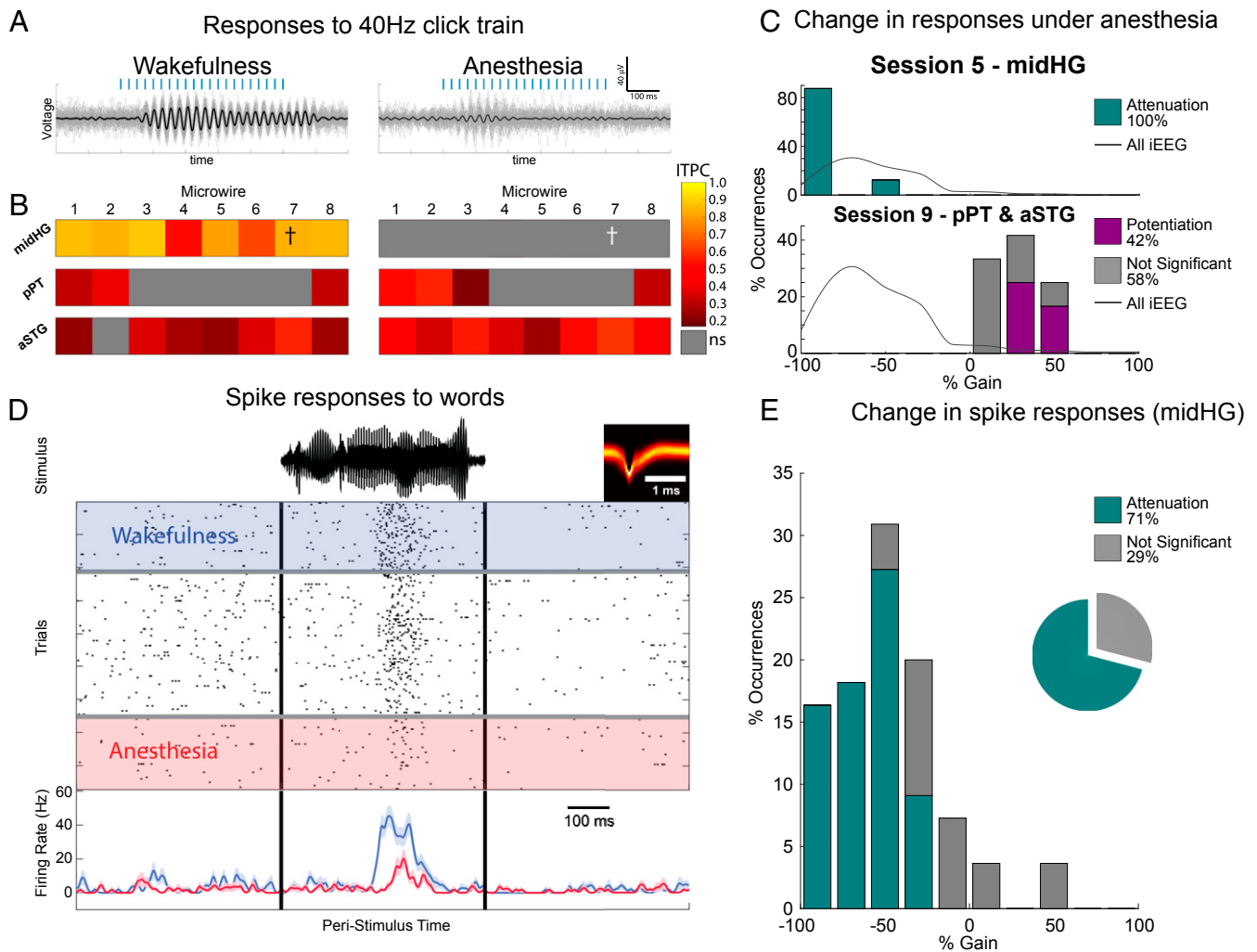

Fig. 4. High-order auditory responses upon anesthetic LOC. (*A*) Band-pass-filtered responses to 40-Hz click train in a representative high-level auditory electrode during wakefulness (*Left*) and anesthesia (*Right*). Thick black traces mark the average responses, while thin gray traces show individual trials. (*B*) Responses (ITPC) to 40-Hz click trains across all high-level auditory microwires ($n = 24$) during wakefulness (*Left*) and anesthesia (*Right*). Cross marks the specific microwire whose responses are shown above, and from which the neuronal unit below (*D*) was recorded. Note attenuation to noise levels upon anesthesia-induced LOC in midHG, and weak potentiation of responses in pPT and aSTG. (*C*) Histograms of response gain under anesthesia for all 20 responding higher auditory microwires (midHG, top and pPT and aSTG) showing either mainly potentiation (purple) or attenuation (cyan bars) depending on the region. This is in contrast to the marked inhibition seen across the brain in iEEG contacts (gray curve). (*D*) Raster plot and peristimulus time histogram (PSTH, below) of representative higher auditory cortex (midHG) neuronal response to a word (stimulus waveform on top in black). Rows (top to bottom) mark individual trials during deepening propofol anesthesia. Blue shading and time course, wakefulness; red shading and time-course, anesthesia. (*E*) Quantitative analysis across all of the high-level auditory responses from the same midHG region ($n = 55$ in eight neurons) reveals that 71% of responses were significantly attenuated and none were significantly potentiated. Note that this attenuation is in line with the changes in ITPC to 40 Hz from the same region shown above.

www.manaraa.com

these regions (*SI Appendix*, Fig. S8, *Bottom Right*) were moderately potentiated, agreeing with the LFP results. Altogether, the effects of anesthetic LOC in higher-order auditory regions were variable (representing either interregional or intersubject variability), but the strongest high-fidelity responses and corresponding spiking activities were significantly attenuated.

Induced Power Responses to Words during Wakefulness and upon Anesthetic LOC. Induced gamma-band (40 to 200 Hz) power is an established and widely used proxy for neuronal activity in local neuronal populations (50). We therefore sought to measure how anesthetic LOC affected gamma power induced by words in both iEEG and LFP signals. We identified 50 iEEG contacts and 34 microwires that showed a significant gamma response in either wakefulness or anesthesia ($P < 0.005$, WSRT, *Materials and Methods*), all of which were located in the temporal lobe (Fig. 5). Fig. 5*A* shows a representative induced power response in an iEEG electrode. Upon anesthetic LOC, the gamma response increased its power and decreased its peak spectral frequency, and the concomitant decrease in power below 20 Hz [often referred to as alpha/beta desynchronization (51)] was largely absent. A quantitative analysis across the entire dataset (*Materials and Methods*) confirmed that increased gamma power was a robust phenomenon across auditory-responsive electrodes [Fig. 5 *B–D*; for iEEG: 83% increase, $P < 10^{-8}$ by WSRT, z(n_{iEEGs} = 50) = 6.02, Cohen's d_z = 1.19, median changes from 0.76 to 1.53 dB; for LFP: 32% increase, $P = 2 \times 10^{-4}$, z(n_{LFPs} = 34) = 3.79, Cohen's d_z = 0.40, median changes from 1.34 to 1.62 dB]. Such consistent increase in gamma power upon anesthetic LOC stands in contrast to changes in neuronal firing rates or time-locked LFP responses to 40-Hz click trains, which often showed attenuation. A decrease in peak gamma spectral frequency was also consistently evident across electrodes (Fig. 5 *B* and *E*; 50-Hz mean shift, $P < 10^{-7}$ by WSRT, z = 5.40, Cohen's d_z = 0.82, median changes from 80 to 50 Hz for iEEGs; 48 Hz mean shift, $P = 3 \times 10^{-5}$, z = 4.14, Cohen's d_z = 0.76, median changes from 84 to 46 Hz for LFPs). Finally, upon LOC the 10- to 20-Hz power decrease (alpha/beta desynchronization) was consistently reduced in iEEG data [Fig. 5 *B*, *Left*; $P = 8 \times 10^{-4}$ by WSRT, z(n = 50) = 3.34, Cohen's d_z = 0.57, median changed from -0.84 to -0.19 dB], but a significant reduction was not observed in LFPs [Fig. 5 *B*, *Right*; $P = 0.83$ by WSRT, z(n = 34) = 0.21, Cohen's d_z = 0.05, median changed from -0.90 to -1.08 dB]. Taken together, anesthetic LOC causes complex changes in induced power including gamma power increase and slowing of spectral frequency profiles, which can be decoupled from local spiking activities after LOC (see also *Discussion*).

Discussion

By studying human auditory responses during the descent to anesthesia, we show that anesthesia-induced LOC is associated with robust disruption of auditory responses in association cortex, while significant early PAC responses persist. LOC was consistently associated with response breakdown across wide cortical territories (Fig. 2 and *SI Appendix*, Figs. S4 and S5). By contrast, both LFP and spike responses in PAC (Fig. 3) consistently showed robust responses after LOC. The distinction between PAC and association cortices was evident in response to both simple 40-Hz click trains and complex word stimuli. In intermediate high-order auditory regions effects were variable, and spiking responses largely attenuated around LOC (Fig. 4). Interestingly, gamma power induced by words increased after LOC while its frequency profile slowed, but such power increase did not correlate with changes in neuronal firing on the same microwires.

Since the study was conducted in neurosurgical epilepsy patients, it inherently entails some limitations that should be explicitly acknowledged. We cannot completely rule out the contribution of epileptogenic activity. In addition, the number of participants implanted with

electrodes in auditory regions that volunteer to participate in research during brain surgery is limited, as is the number of recorded neurons. However, the highly consistent results across patients with different clinical profiles largely overcome these limitations. Another possible concern is that the precise brain regions targeted and the anesthesia protocols vary between sessions, as they are guided by clinical criteria. We addressed this by employing a within-session design and defining the anesthesia interval according to the same criterion (loss of responsiveness on the behavioral task) across all sessions. Furthermore, the same anesthetic agent (propofol) was used for all sessions. Future studies will determine the extent to which these findings generalize to other anesthetic agents.

While we acknowledge that it is difficult to distinguish LOC from unresponsiveness once someone does not respond, we believe that, overall, the anesthesia state we focus on here represents LOC rather than mere unresponsiveness. We observed multiple features that match those reported in many previous studies investigating anesthetic LOC (33, 40–44, 46), including the dynamics of behavioral performance on the task, iEEG power changes, clinical assessment of ongoing behavior (including responses to sporadic painful stimuli that were either entirely absent or reflexive at most), and anesthetic drug infusion details.

In contrast to the "thalamic gating" hypothesis whereby the relay to primary sensory regions is disrupted (38), our results support the notion of preserved thalamocortical connectivity (42, 43) and PAC responses under light anesthesia (29, 33, 52), as was also found for LFP responses to visual stimulation (21). Two recent studies examining the effects of propofol on human LFP auditory responses reported preserved early-evoked potentials in the most posteromedial part of Heschl's gyrus when compared to intermediate and anterolateral regions showing robust attenuation (53), as well as preservation of novelty responses over short (local deviant) time scales in auditory cortex (54). Our study extends these observations along several dimensions, most importantly by recording spike responses to complex word stimuli. The contribution of these data are twofold. First, it consistently showed effects similar to LFP ITPC results, thereby allowing us to extrapolate and confidently interpret time-locked LFP responses as reflecting local spiking activities even when these were not available. Second, it exposed interesting differences after LOC compared with simultaneously recorded gamma power changes. The fact that spiking responses are preserved in PAC is of particular importance since this demonstrates unequivocally that during anesthetic LOC not only is the synaptic input into PAC preserved but also the circuit's output. The apparent discrepancy with studies reporting attenuation of PAC responses under anesthesia (26–28) may reflect effects of deep surgical anesthesia unrelated to LOC, and highlights the importance of using "just-hypnotic" anesthesia when studying LOC. While the present results establish preserved PAC responses to isolated stimuli upon anesthesia-induced LOC, they do not preclude potential effects on select neuronal populations, precise spike timing, or contextual effects that require integration across long temporal intervals.

Attenuated EEG responses to 40-Hz click trains have been repeatedly demonstrated upon anesthesia-induced LOC and have been suggested as a useful marker for assessing the depth of anesthesia (31, 55). Our results indicate that disruption of scalp EEG responses represent attenuated activity in association cortices, as can be expected given that preserved PAC responses only modestly contribute to total cerebral activity, and given the medial location of PAC that is less accessible to noninvasive scalp EEG. Indeed, our own iEEG results show robust attenuation upon anesthesia-induced LOC (Fig. 2). The effectiveness of the specific 40-Hz click-train stimulus in revealing correlations with LOC may be related to an inability of large neuronal populations to reliably synchronize coherently with high-frequency
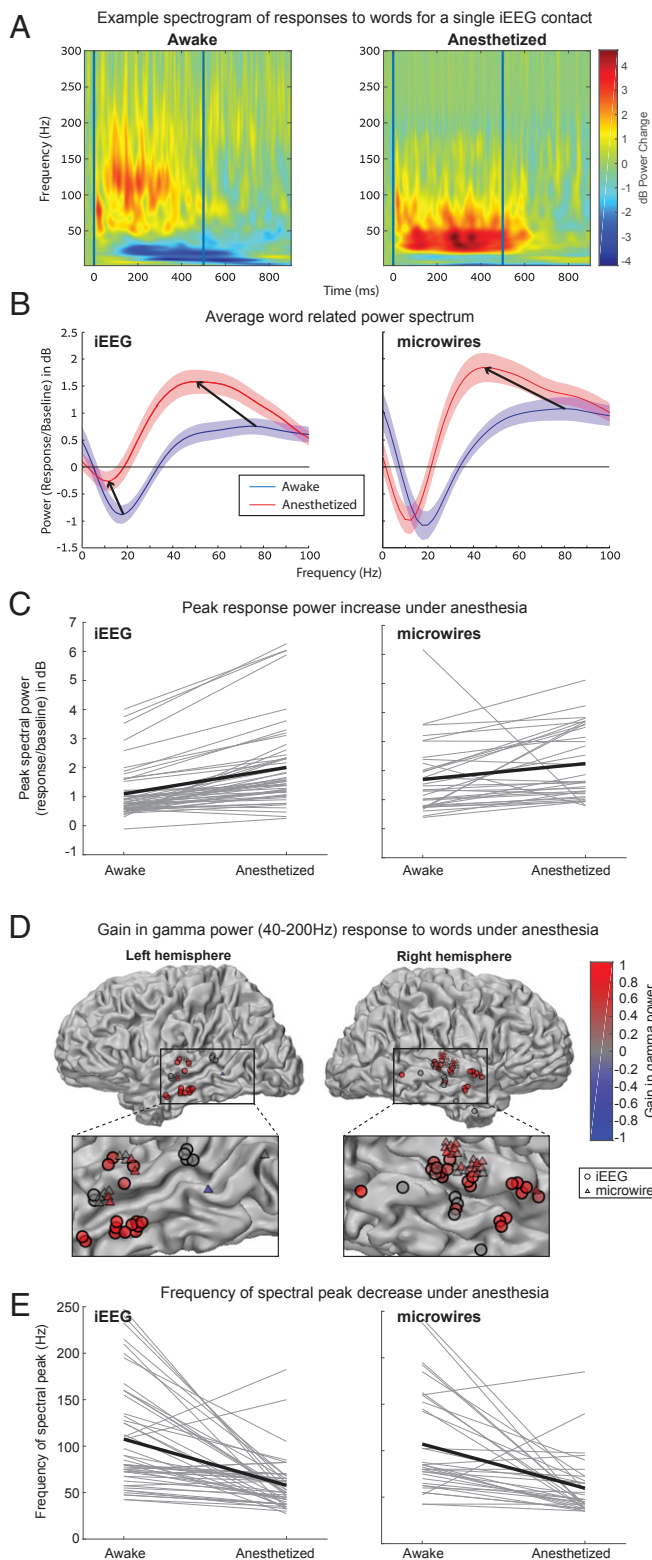
Fig. 5. Induced gamma power responses to words upon anesthetic LOC. (*A*) Example of a single temporal lobe iEEG contact ERSP averaged across words, demonstrating an increase in peak power, a reduction in the frequency of the power peak, and reduction in alpha/beta desynchronization, under anesthesia. (*B*) The power spectrum averaged over all 50 significantly responding (*P* < 0.005) iEEG contacts (*Left*) and all 34 significantly responding microwires (*Right*) shows the same increase in peak power and shift to lower frequencies of the power peak. The iEEG spectrum also shows the reduction in alpha/beta desynchronization noted above. The peak power (*C*) and frequency of the

stimulation in disconnected states (56). Studies in natural sleep demonstrate a similar distinction between preserved tracking of acoustic properties and PAC responses (57) vs. high-order activity in association cortex (58). Thus, a functional disconnection between primary sensory and association cortex may be a general property of LOC not only due to anesthesia, as demonstrated also by direct perturbation of cortical activity with transcranial magnetic stimulation (59–61). In addition, our results join findings from other lines of research showing that when sensory stimuli are not perceived, activity in primary sensory regions is largely preserved whereas activity in association cortices is attenuated (43, 62–65).

Our findings reveal complex effects on induced power changes, where anesthetic LOC was associated with gamma power increase and a slowing of frequency profiles (Fig. 5). Such changes are in line with previous studies showing that anesthesia/sedation increases gamma responses power in vitro (66) and in humans in vivo (67, 68). Similarly, a slowing of spectral frequencies upon anesthesia has been observed in vitro (66, 69) and in monkeys (70) and humans in vivo (68). While induced gamma power usually accompanies neuronal spiking activity (50), our results show that the relation between induced gamma power and local spiking activity may change across states. The extent of potential decoupling between gamma activity and neuronal firing remains unclear, and we can only speculate about its underlying source. One possibility is that these two measures emphasize the contribution of different neuronal populations that diverge upon anesthetic LOC. For example, gamma oscillations are closely coupled with inhibitory GABAergic interneurons (71), while extracellular recordings mostly capture excitatory pyramidal cells (72). Differences may also stem from differential contributions from distinct cortical layers or cell populations at different spatial scales. We also find that stimulus-induced decrease in 10- to 20-Hz power (prevalent during wakefulness) diminishes upon anesthetic LOC (Fig. 5). Given that alpha/beta desynchronization has been linked with top-down signaling (73), this may support the notion that anesthesia predominantly affects top-down signaling (29, 74).

What could be the mechanisms by which LOC disrupts cortical functional connectivity? As noted in the Introduction, anesthesia may act at multiple subcortical mechanisms simultaneously (2, 9, 11–13, 15, 75) in a manner that ultimately results in reduced cortical connectivity. For example, anesthesia may exert its effects by affecting endogenous subcortical sleep/wake neuromodulation centers that modify thalamocortical activity (2, 13). Accordingly, the distribution of modulatory receptors may differ between primary sensory regions and association cortices, rendering the latter unresponsive to preserved ascending input. An alternative explanation for the inability to effectively drive responses in association cortices may reflect a disruption to indirect cortico-thalamo-cortical pathways linking cortical regions via high-order thalamic nuclei (76, 77). Thus, refining the traditional "thalamic gating" notion from disruption of primary relay nuclei, to focus on high-order thalamic nuclei, could reconcile the present results with the well-established effect of anesthesia reducing thalamic activity (38). Alternatively, our findings may reflect a "multiple hit mechanism," whereby anesthesia causes multiple small perturbations at each step in the sensory processing chain. The sum of these perturbations may seem modest in the PAC as measured with current methods but may have accumulated sufficiently to be noticeable in the higher association cortices. Finally,

power peak (*E*) plotted for each individual responding iEEG contact/microwire shows that these changes are consistent across contacts. (*D*) Plot of all 50 responding iEEG contacts and 34 responding microwires colored according to gain in gamma power under anesthesia. Responses are clustered exclusively around the temporal lobe and in 83/84 cases show increased power or no change.

anesthetics could affect top-down signaling that may be more dominant in association cortices (74, 78), possibly involving specific ion channels that link bottom-up and top-down signaling (79). Furthermore, anesthetic agents may employ several of these mechanisms in parallel since they reach much of the brain and central nervous system almost simultaneously. Beyond the specific mechanisms at play, the disruption of effective cortical connectivity is consistent with a number of theoretical perspectives (80, 81).

In conclusion, our findings demonstrate that anesthesia-induced LOC disrupts auditory responses beyond primary cortex while significant responses persist in PAC. The fact that the major disruption in sensory signaling upon LOC occurs after primary cortices highlights impaired effective cortical connectivity as a key factor in LOC, a factor that should guide future mechanistic research of LOC, development of anesthetic agents, and design of depths of anesthesia monitoring schemes.

Materials and Methods

Subjects. Eight patients (six male; see *SI Appendix*, Table S1 for details) with intractable drug-resistant epilepsy were implanted with chronic depth electrodes, or subdural cortical grids and strips (one session), for 7 to 10 d, to identify seizure foci for potential surgical treatment. Electrode location and anesthesia management (discussed below) were based solely on clinical criteria. One patient was implanted on two different occasions due to inconclusive clinical results from the first hospital admission. All patients provided written informed consent to participate in the research study. This study was approved by the Institutional Review Board at Tel Aviv Sourasky Medical Center and the University of Bonn Epileptology Department (one individual). Data were collected prior to removal of the electrodes under anesthesia at the end of monitoring on the medical ward.

Anesthesia. Standard anesthesia monitoring was performed according to the guidelines set by the ASA, complemented with bispectral index monitoring (49) (BIS VISTA Monitoring System; Medtronic). Propofol was infused using a simple (non-target controlled infusion) syringe pump, with infusion rates increasing in a stepwise fashion over 20 to 40 min [to a maximum of 45 to 400 μg/(kg·min) depending on the patient and according to the judgment of the anesthesiologist]) to achieve anesthesia while maintaining spontaneous ventilation. In two sessions (*SI Appendix*, Table S1) adjuvant agents (fentanyl, midazolam, or remifentanil) were given according to clinical considerations. When a sufficient depth of anesthesia was achieved (aiming to avoid movement in response to painful stimulus while maintaining spontaneous ventilation), the neurosurgeons removed the electrodes. Post hoc pharmacokinetic and pharmacodynamic modeling using the three-compartment Marsh model (82–85) (*SI Appendix*, Fig. S1) were used to estimate the momentary effect-site concentration of propofol in brain tissue (Fig. 1 and *SI Appendix*, Fig. S2).

Auditory Paradigm. Auditory stimuli were continuously presented throughout the descent to anesthesia (20 to 70 min) using headphones (eight sessions) or speakers (one session), with sound intensity levels adjusted at the start of each session to be comfortably audible. 40-Hz click trains (duration = 500 ms, 21 clicks) were presented in all recording sessions. Additionally, up to seven word stimuli (duration = 500 to 600 ms), including one task target (duration 500 ms), were presented in seven sessions. Auditory stimuli were presented in a pseudorandom order, at 1.5-s intervals (± 400-ms jitter). Patients were instructed to press a response button upon hearing a specific target word, to determine the moment of loss of responsiveness under anesthesia.

Electrophysiology. In eight sessions, patients had been implanted with 5 to 11 depth electrodes targeting different brain regions (Fig. 1*B*), whereby each electrode consisted of eight platinum iEEG contacts along their shaft, eight additional microwires protruding a few millimeters from the distal tip, and a ninth low-impedance reference microwire (86). In one of these sessions only iEEG data were available. In a separate ninth session, a patient was implanted with a combination of two two-dimensional subdural electrocorticography (ECoG) grid arrays and four one-dimensional subdural ECoG strips (i.e., instead of depth electrodes). Data were recorded using either Blackrock or Neuralynx data acquisition systems. Microwire data were sampled at 30 kHz (Blackrock) or 32,768 Hz (Neuralynx) and referenced to the local low-impedance ninth microwire on each electrode, or in one session to a single low-impedance ninth microwire (session 6; *SI Appendix*, Table S1). iEEG and ECoG data were sampled at 2 kHz (Blackrock) or 2,048 Hz (Neuralynx) and referenced to a central scalp electrode (Cz).

Electrode Localization. Preimplant MRI scans (Siemens Prisma scanner or GE Signa scanner, 3 T, T1 sequence, resolution 1 mm × 1 mm × 1 mm) were coregistered with postimplant computed tomography (CT) scans (Philips MX8000 or Brilliance, resolution 1.5 mm × 0.5 mm × 0.5 mm or 0.75 mm × 0.5 mm × 0.5 mm) to identify locations of electrodes. Individual subject data were further transformed into Talairach space (87) to facilitate simultaneous visualization of electrode positions in different individuals. To this end, electrode locations were marked with 5-mm spheres on the standard brain, and intersections with the gray–white matter boundary surface were identified. The cortical surface was then inflated and flattened by unfolding and cutting along the calcarine sulcus and predefined medial anatomical landmarks (*SI Appendix*, Fig. S4). When plotted on folded gray–white matter boundary surface (Figs. 2 and 5 and *SI Appendix*, Fig. S5), the location of each electrode was defined as the center of mass of the intersection of the 5-mm sphere with the surface, and a circle was drawn in that location (minimal jitter was introduced to allow visualization and avoid hidden data).

Defining "Wakefulness" vs. "Anesthesia" Periods and State Characterization. To compare auditory responses during propofol-free wakefulness to those under light anesthesia [formally defined by the ASA as "deep sedation": unresponsiveness to simple verbal instructions, or modified Ramsay score >3: no purposeful response to commands at conversational level (45)] we defined the anesthesia period as the first 8 min following loss of responsiveness (a proxy for LOC). In order to avoid excessively deep anesthesia, we confirmed that BIS values remained above 50 (49). *SI Appendix*, Table S1 and Fig. S2 provide full details regarding recording durations and definitions of wakefulness and anesthesia intervals in each session. Loss of responsiveness was defined as the midpoint between the last correct response to the target word and the following missed target word. Consideration was given to assessing depth of anesthesia according to responses to intermittently delivered, graded severity of stimuli [e.g., the Observer's Assessment of Alertness/Sedation Scale (88)], which involves "mild prodding/shaking," or the modified Ramsay Sedation Scale (45) involving loud commands and painful stimuli), which would have allowed a more precise assessment of depth of sedation. However, such stimulation can itself wake subjects from shallow states of unconsciousness (89) and give a false measurement of alertness, and so we chose to rely on unprompted performance in the word identification task described above. In sessions 1, 2, and 7 where it was not possible to characterize responsiveness based on behavioral button press data, we defined loss of responsiveness as the time when the patient was observed to stop reacting purposefully to his environment, by noting for example when he stopped talking to caregivers or when he responded only to painful stimuli (applied incidentally by clinicians) such as scalp scrubbing or needle sticks. While it was not our intention to assess responses to pain, in four sessions (sessions 1, 2, 5, and 9) the clinicians applied a painful stimulus (scalp scrubbing or jaw thrust) after the end of our defined anesthesia period. On half of these occasions (sessions 1 and 9) the patient responded with reflexive hand movement (modified Ramsay = 7) while in the other two there was no movement (modified Ramsay = 8). For each experimental session, we chose an interval of propofol-free wakefulness with identical duration for a within-session comparison. In two sessions the anesthesia period was truncated to avoid deep anesthesia (sessions 7 and 8), defined by BIS <50. Whenever eight minutes were not available for either wakefulness or anesthesia, we used the longest possible noise-free intervals with identical durations in both wakefulness and anesthesia (*SI Appendix*, Fig. S2 and Table S1). Average BIS values quoted in the text were calculated by integrating over BIS curves during wakefulness or anesthesia for each session (with linear interpolation between known data points), and then taking the median across sessions. In all but one session, patients breathed spontaneously and maintained their airways throughout the period defined as anesthesia. In session 2 the patient required a jaw thrust and Guedel oral airway to maintain his airway.

State characterizations (Fig. 1 *G–I*) of frontal iEEG power changes, behavioral performance, and additional anesthesia depth features were performed for three session periods: wakefulness, 4 min of noise-free transition just before LOC, and anesthesia (defined above). Mean power changes relative to wakefulness (spectrogram in Fig. 1*G*, n = 7 sessions with frontal iEEG) were obtained using short-time Fourier transform (2-s window) and smoothed with a two-dimensional Gaussian kernel (σ_{time} = 10 s, $\sigma_{frequency}$ = 1 Hz). Statistical comparisons between these periods (Fig. 1*H*) were performed for frontal iEEG alpha (8 to 12 Hz) and delta (0.3 to 4 Hz) power changes (n = 7 sessions with frontal iEEG) and behavioral task performance (% hit rate, n = 7 session with behavioral task data) using a WSRT.

Krom et al.

www.manaraa.com

Analysis of iEEG/LFP Responses to 40-Hz Click Trains. Responses to 40-Hz click trains were quantified using ITPC (Figs. 2 and 3), also known as the "phase-locking factor" (90, 91):

$$ITPC = \left| \frac{1}{N} \sum_{k=1}^{N} e^{i\phi_k} \right|,$$

where N signifies the number of trials and ϕ_k the phase of the spectral estimate for trial k for the 40-Hz frequency. This phase for each trial was estimated as the angle of the Fourier transform component at 40 Hz of the entire stimulus duration iEEG/LFP response, following application of a Hann window.

The statistical significance values associated with ITPC were estimated as in Zar (92) with a significance threshold of $\alpha = 0.01$:

$$p = \exp\left[\sqrt{1 + 4N + 4(N^2 - ITPC^2)} - (1 + 2N)\right],$$

where N is the number of trials and ITPC is the calculated ITPC.

Quoted averages of ITPC P values are the median of these P value estimates. Median ITPC values for *SI Appendix*, Fig. S4 were calculated on the 421 iEEG electrodes showing significant ITPC in either wakefulness or anesthesia.

The gain factor between wakefulness and anesthesia was calculated as in as in refs. 57 and 93:

$$Gain = \frac{R_{Anesthetized} - R_{Awake}}{\max(|R_{Anesthetized}|, |R_{Awake}|)},$$

where $R_{Anesthetized}$ and R_{Awake} are the ITPC for a particular channel during wakefulness or anesthesia. We obtained largely similar results when calculating gains using only R_{Awake} in the denominator (not shown). Additionally, responses were quantified by calculating the ERSP at 40 Hz (*SI Appendix*, Figs. S5 and S7), reflecting power modulations that are not necessarily phase-locked and known also as "induced power." To this end, the 40-Hz spectral power was calculated by applying a Hann window over the 500 ms of the response (or baseline) iEEG/LFP signal and calculating the squared 40-Hz amplitude component of the Fourier transform. Spectral power during baseline was subtracted from that during response and the result divided by the median baseline spectral power at 40 Hz. This ERSP was averaged across all trials for each electrode (*SI Appendix*, Figs. S5 and S7). Statistical significance of ERSP responses was calculated using WSRT, with significance level of $\alpha = 0.01$ (nonsignificant values are masked in gray in *SI Appendix*, Fig. S5). *Response latency.* Latency (*SI Appendix*, Fig. S6B) was calculated based on the locally referenced LFP response to the 40-Hz click train during wakefulness for each individual microwire targeted around Heschl's gyrus (Figs. 3 and 4). We identified the stereotypic response to the 40-Hz click train, consisting of a 40-Hz oscillation with exactly 21 peaks (matching the 21 clicks in the click train), and obtained each individual microwire's latency as the onset of this stereotypic response after convolving the 40-Hz response envelope with a 525-ms square window. This method requires responses to be strongly coherent between trials and was possible to implement in 72% of auditory-responsive electrodes with ITPC >0.5 (most of which were >0.85). The mean LFP response ([−600, 2,000] ms from stimulus onset) to 40-Hz click train was bandpassed at 30 to 150 Hz (fourth-order zero-phase-shift digital butterworth filter) to include the LFP response at 40 Hz and its harmonics. Then, its envelope was extracted using the Hilbert transform. Using a 525-ms-length moving window (window size was chosen to match the LFP response to the stimulus of 21 clicks with 25-ms interspike interval, ISI), latency was defined as the onset time of the window where the largest mean envelope was obtained.

LFP-induced power response to words. Responses were quantified by measuring, for each microwire and iEEG contact, the event-related gamma power (40 to 200 Hz, mean of Fast Fourier Transform magnitudes squared) for each trial across words (100- to 500-ms Hann window, posttrial onset) and comparing it with power during the corresponding prestimulus baseline period (−450 to −50 ms). "Responding channels" were defined as those in which this gamma power during response was significantly different from baseline gamma power ($P < 0.005$, WSRT) and were selected for further analysis. Response power spectra for each responding channel were calculated by dividing the event-related power in each trial (100 to 500 ms) at each frequency by the corresponding baseline power and then taking the median across wakefulness (or anesthesia) trials. This spectrum per channel was then averaged (mean ± SEM) across iEEG or microwire channels to visualize the grand mean profile (Fig. 5B). The peak spectral power during wakefulness or anesthesia was determined for each channel separately by identifying the highest peak in the power spectrum and finding its power (Fig. 5C) and frequency (Fig. 5E). The alpha/beta desynchronization trough power during wakefulness or anesthesia was determined for each channel by identifying the deepest trough in the power spectrum that was to the left of (lower frequency than) the peak power above, and which also lay below 50 Hz. On occasions where no such trough was identified, the alpha/beta desynchronization was assumed to have disappeared, and the trough value was set to 0 dB. Gain factors between wakefulness and anesthetic LOC for gamma power (Fig. 5D) were calculated in each channel separately as follows. Event-related gamma power change compared to baseline (as described above) was normalized by dividing by the median baseline power across trials, and averaged over awake (or anesthesia) trials, yielding a "gamma power response" for that channel during wakefulness (or anesthesia). The gain factor was then calculated as described above for ITPC, but substituting $R_{Anesthetized}$ and R_{Awake} with the gamma power response for a particular channel during wakefulness or anesthesia.

Analysis of Neuronal Spiking Activity. Spike sorting was performed using the wave_clus toolbox for MATLAB as described previously (94, 95): 1) extracellular microwire recordings were high-pass-filtered above 300 Hz, 2) a 5 × SD-approximation $(median\{|data|/0.6745\})$ threshold above the median noise level was computed, and 3) detected events were clustered using superparamagnetic clustering and categorized as noise, single- or multiunit clusters. Classification of single- and multiunit clusters was based on the consistency of action potential waveforms, and by the presence of a refractory period for single units, that is, less than 1% of ISIs within 3 ms.

Response components were identified via an automatic algorithm (*SI Appendix*, Fig. S9 and *Text*) and categorized as potentiated, attenuated, or unchanged under anesthesia via WRST with a significance level of $\alpha = 0.05$. *Statistics.* P values were calculated using WRST, WSRT, or Monte Carlo permutation tests, as reported above, while treating iEEG or LFP for different electrodes as independent measures, unless otherwise stated. Effect sizes were quantified using Cohen's d (for unpaired data) and Cohen's d_z (for paired data, mean of the differences divided by their SD). Error bars in all figures denote SEM (SEM = SD/$\sqrt{n}$, where n is the number of data points) unless otherwise stated.

Data and Code Availability. The data that support the findings of this study and the computer code used to generate the results are available from the corresponding author upon reasonable request.

1. H. J. Bigelow, Insensibility during surgical operations produced by inhalation. *Boston Med. Surg. J.* **35**, 309–317 (1846).
2. E. N. Brown, P. L. Purdon, C. J. Van Dort, General anesthesia and altered states of arousal: A systems neuroscience analysis. *Annu. Rev. Neurosci.* **34**, 601–628 (2011).
3. E. N. Brown, R. Lydic, N. D. Schiff, General anesthesia, sleep, and coma. *N. Engl. J. Med.* **363**, 2638–2650 (2010).
4. A. Evers, M. Crowder, "Cellular and molecular mechanisms of anesthesia" in *Clinical Anesthesia*, P. G. Barash, B. F. Cullen, R. K. Stoelting, M. Cahalan, M. C. Stock, Eds. (Lippincott Williams & Wilkins, ed. 6, 2006), pp. 95–114.
5. V. M. Seutin, K. W. Miller, S. A. Forman, Mechanisms of actions of inhaled anesthetics. *N. Engl. J. Med.* **349**, 909–910, author reply 909–910 (2003).
6. H. C. Hemmings, Jr *et al.*, Emerging molecular mechanisms of general anesthetic action. *Trends Pharmacol. Sci.* **26**, 503–510 (2005).
7. U. Rudolph, B. Antkowiak, Molecular and neuronal substrates for general anaesthetics. *Nat. Rev. Neurosci.* **5**, 709–720 (2004).
8. D. Kennedy, C. Norman, What don't we know? *Science* **309**, 75 (2005).
9. N. P. Franks, General anaesthesia: From molecular targets to neuronal pathways of sleep and arousal. *Nat. Rev. Neurosci.* **9**, 370–386 (2008).
10. M. T. Alkire, A. G. Hudetz, G. Tononi, Consciousness and anesthesia. *Science* **322**, 876–880 (2008).
11. J. T. Moore *et al.*, Direct activation of sleep-promoting VLPO neurons by volatile anesthetics contributes to anesthetic hypnosis. *Curr. Biol.* **22**, 2008–2016 (2012).

Krom et al.

12. F. J. Flores et al., Thalamocortical synchronization during induction and emergence from propofol-induced unconsciousness. Proc. Natl. Acad. Sci. U.S.A. 114, E6660–E6668 (2017).

13. M. Devor, V. Zalkind, Reversible analgesia, atonia, and loss of consciousness on bilateral intracerebral microinjection of pentobarbital. Pain 94, 101–112 (2001).

14. A. H. Song et al., Pharmacological modulation of noradrenergic arousal circuitry disrupts functional connectivity of the locus coeruleus in humans. J. Neurosci. 37, 6938–6945 (2017).

15. G. A. Mashour, Consciousness unbound: Toward a paradigm of general anesthesia. Anesthesiology 100, 428–433 (2004).

16. Y. Ishizawa et al., Dynamics of propofol-induced loss of consciousness across primate neocortex. J. Neurosci. 36, 7718–7726 (2016).

17. V. B. Mountcastle, Modality and topographic properties of single neurons of cat's somatic sensory cortex. J. Neurophysiol. 20, 408–434 (1957).

18. D. H. Hubel, T. N. Wiesel, Receptive fields of single neurones in the cat's striate cortex. J. Physiol. 148, 574–591 (1959).

19. M. M. Merzenich, P. L. Knight, G. L. Roth, Representation of cochlea within primary auditory cortex in the cat. J. Neurophysiol. 38, 231–249 (1975).

20. F. Wörgötter et al., State-dependent receptive-field restructuring in the visual cortex. Nature 396, 165–168 (1998).

21. O. A. Imas, K. M. Ropella, B. D. Ward, J. D. Wood, A. G. Hudetz, Volatile anesthetics disrupt frontal-posterior recurrent information transfer at gamma frequencies in rat. Neurosci. Lett. 387, 145–150 (2005).

22. B. Haider, M. Häusser, M. Carandini, Inhibition dominates sensory responses in the awake cortex. Nature 493, 97–100 (2013).

23. I. Ferezou, S. Bolea, C. C. H. Petersen, Visualizing the cortical representation of whisker touch: Voltage-sensitive dye imaging in freely moving mice. Neuron 50, 617–629 (2006).

24. C. M. Constantinople, R. M. Bruno, Effects and mechanisms of wakefulness on local cortical networks. Neuron 69, 1061–1068 (2011).

25. D. Kleinfeld, E. Ahissar, M. E. Diamond, Active sensation: Insights from the rodent vibrissa sensorimotor system. Curr. Opin. Neurobiol. 16, 435–444 (2006).

26. J. F. Brugge, M. M. Merzenich, Responses of neurons in auditory cortex of the macaque monkey to monaural and binaural stimulation. J. Neurophysiol. 36, 1138–1158 (1973).

27. E. F. Evans, I. C. Whitfield, Classifcation of unit responses in the auditory cortex of the unanaesthetized and unrestrained cat. J. Physiol. 171, 476–493 (1964).

28. Y. Katsuki, K. Murata, N. Suga, T. Takenaka, Electrical activity of cortical auditory neurons of unanaesthetized and unrestrained cat. Proc. Jpn. Acad. 35, 571–574 (1959).

29. A. Raz et al., Preferential effect of isoflurane on top-down vs. bottom-up pathways in sensory cortex. Front. Syst. Neurosci. 8, 191 (2014).

30. D. Schwender, S. Klasing, C. Madler, E. Pöppel, K. Peter, Depth of anesthesia. Mid-latency auditory evoked potentials and cognitive function during general anesthesia. Int. Anesthesiol. Clin. 31, 89–106 (1993).

31. G. Plourde, The effects of propofol on the 40-Hz auditory steady-state response and on the electroencephalogram in humans. Anesth. Analg. 82, 1015–1022 (1996).

32. M. H. Dueck et al., Propofol attenuates responses of the auditory cortex to acoustic stimulation in a dose-dependent manner: A fMRI study. Acta Anaesthesiol. Scand. 49, 784–791 (2005).

33. M. H. Davis et al., Dissociating speech perception and comprehension at reduced levels of awareness. Proc. Natl. Acad. Sci. U.S.A. 104, 16032–16037 (2007).

34. W. Heinke et al., Sequential effects of propofol on functional brain activation induced by auditory language processing: An event-related functional magnetic resonance imaging study. Br. J. Anaesth. 92, 641–650 (2004).

35. V. C. Austin et al., Confounding effects of anesthesia on functional activation in rodent brain: A study of halothane and α-chloralose anesthesia. Neuroimage 24, 92–100 (2005).

36. W. Heinke, C. Schwarzbauer, In vivo imaging of anaesthetic action in humans: Approaches with positron emission tomography (PET) and functional magnetic resonance imaging (fMRI). Br. J. Anaesth. 89, 112–122 (2002).

37. R. R. Llinás, M. Steriade, Bursting of thalamic neurons and states of vigilance. J. Neurophysiol. 95, 3297–3308 (2006).

38. M. T. Alkire, R. J. Haier, J. H. Fallon, Toward a unified theory of narcosis: Brain imaging evidence for a thalamocortical switch as the neurophysiologic basis of anesthetic-induced unconsciousness. Conscious. Cogn. 9, 370–386 (2000).

39. L. D. Lewis et al., Rapid fragmentation of neuronal networks at the onset of propofol-induced unconsciousness. Proc. Natl. Acad. Sci. U.S.A. 109, E3377–E3386 (2012).

40. P. L. Purdon et al., Electroencephalogram signatures of loss and recovery of consciousness from propofol. Proc. Natl. Acad. Sci. U.S.A. 110, E1142–E1151 (2013).

41. R. Ní Mhuircheartaigh, C. Warnaby, R. Rogers, S. Jbabdi, I. Tracey, Slow-wave activity saturation and thalamocortical isolation during propofol anesthesia in humans. Sci. Transl. Med. 5, 208ra148 (2013).

42. P. Boveroux et al., Breakdown of within- and between-network resting state functional magnetic resonance imaging connectivity during propofol-induced loss of consciousness. Anesthesiology 113, 1038–1053 (2010).

43. G. G. Supp, M. Siegel, J. F. Hipp, A. K. Engel, Cortical hypersynchrony predicts breakdown of sensory processing during loss of consciousness. Curr. Biol. 21, 1988–1993 (2011).

44. M. Murphy et al., Propofol anesthesia and sleep: A high-density EEG study. Sleep 34, 283–91A (2011).

45. M. Gill, S. M. Green, B. Krauss, A study of the Bispectral Index Monitor during procedural sedation and analgesia in the emergency department. Ann. Emerg. Med. 41, 234–241 (2003).

46. H. Iwakiri et al., Individual effect-site concentrations of propofol are similar at loss of consciousness and at awakening. Anesth. Analg. 100, 107–110 (2005).

47. E. A. Mukamel et al., A transition in brain state during propofol-induced unconsciousness. J. Neurosci. 34, 839–845 (2014).

48. ASA, "Continuum of depth of sedation: Definition of general anesthesia and levels of sedation/analgesia" (American Society of Anesthesiologists, 2019).

49. S. D. Kelley, Monitoring Consciousness Using the Bispectral Index Using the Bispectral Index during Anesthesia (Covidien, Boulder, CO, ed. 2, 2010).

50. Y. Nir et al., Coupling between neuronal firing rate, gamma LFP, and BOLD fMRI is related to interneuronal correlations. Curr. Biol. 17, 1275–1285 (2007).

51. G. Pfurtscheller, A. Aranibar, Event-related cortical desynchronization detected by power measurements of scalp EEG. Electroencephalogr. Clin. Neurophysiol. 42, 817–826 (1977).

52. X. Liu et al., Propofol disrupts functional interactions between sensory and high-order processing of auditory verbal memory. Hum. Brain Mapp. 33, 2487–2498 (2012).

53. K. V. Nourski et al., Electrocorticographic delineation of human auditory cortical fields based on effects of propofol anesthesia. Neuroimage 152, 78–93 (2017).

54. K. V. Nourski et al., Auditory predictive coding across awareness states under anesthesia: An intracranial electrophysiology study. J. Neurosci. 38, 8441–8452 (2018).

55. A. Yli-Hankala, H. L. Edmonds, Jr, M. F. Heine, T. Strickland,, Jr, K. Tsueda, Auditory steady-state response, upper facial EMG, EEG and heart rate as predictors of movement during isoflurane-nitrous oxide anaesthesia. Br. J. Anaesth. 73, 174–179 (1994).

56. O. Sharon, Y. Nir, Attenuated fast steady-state visual evoked potentials during human sleep. Cereb. Cortex 28, 1297–1311 (2018).

57. Y. Nir, V. V. Vyazovskiy, C. Cirelli, M. I. Banks, G. Tononi, Auditory responses and stimulus-specific adaptation in rat auditory cortex are preserved across NREM and REM sleep. Cereb. Cortex 25, 1362–1378 (2015).

58. S. Makov et al., Sleep disrupts high-level speech parsing despite significant basic auditory processing. J. Neurosci. 37, 7772–7781 (2017).

59. M. Massimini et al., Breakdown of cortical effective connectivity during sleep. Science 309, 2228–2232 (2005).

60. F. Ferrarelli et al., Breakdown in cortical effective connectivity during midazolam-induced loss of consciousness. Proc. Natl. Acad. Sci. U.S.A. 107, 2681–2686 (2010).

61. S. Sarasso et al., Consciousness and complexity during unresponsiveness induced by propofol, xenon, and ketamine. Curr. Biol. 25, 3099–3105 (2015).

62. R. Blake, N. Logothetis, Visual competition. Nat. Rev. Neurosci. 3, 13–21 (2002).

63. D. A. Leopold, N. K. Logothetis, Activity changes in early visual cortex reflect monkeys' percepts during binocular rivalry. Nature 379, 549–553 (1996).

64. S. Sachidhanandam, V. Sreenivasan, A. Kyriakatos, Y. Kremer, C. C. H. Petersen, Membrane potential correlates of sensory perception in mouse barrel cortex. Nat. Neurosci. 16, 1671–1677 (2013).

65. H. Gelbard-Sagiv, E. Magidov, H. Sharon, T. Hendler, Y. Nir, Noradrenaline modulates visual perception and late visually evoked activity. Curr. Biol. 28, 2239–2249.e6 (2018).

66. O. O. Oke et al., High-frequency gamma oscillations coexist with low-frequency gamma oscillations in the rat visual cortex in vitro. Eur. J. Neurosci. 31, 1435–1445 (2010).

67. N. Saxena et al., Enhanced stimulus-induced gamma activity in humans during propofol-induced sedation. PLoS One 8, e57685 (2013).

68. D. Lozano-Soldevilla, N. ter Huurne, R. Cools, O. Jensen, GABAergic modulation of visual gamma and alpha oscillations and its consequences for working memory performance. Curr. Biol. 24, 2878–2887 (2014).

69. M. A. Whittington, J. G. Jefferys, R. D. D. D. Traub, Effects of intravenous anaesthetic agents on fast inhibitory oscillations in the rat hippocampus in vitro. Br. J. Pharmacol. 118, 1977–1986 (1996).

70. D. Xing et al., Stochastic generation of gamma-band activity in primary visual cortex of awake and anesthetized monkeys. J. Neurosci. 32, 13873–13880a (2012).

71. M. Bartos, I. Vida, P. Jonas, Synaptic mechanisms of synchronized gamma oscillations in inhibitory interneuron networks. Nat. Rev. Neurosci. 8, 45–56 (2007).

72. I. V. Viskontas, A. D. Ekstrom, C. L. Wilson, I. Fried, Characterizing interneuron and pyramidal cells in the human medial temporal lobe in vivo using extracellular recordings. Hippocampus 17, 49–57 (2007).

73. T. van Kerkoerle et al., Alpha and gamma oscillations characterize feedback and feedforward processing in monkey visual cortex. Proc. Natl. Acad. Sci. U.S.A. 111, 14332–14341 (2014).

74. G. A. Mashour, Top-down mechanisms of anesthetic-induced unconsciousness. Front. Syst. Neurosci. 8, 115 (2014).

75. G. A. Mashour, Cognitive unbinding: A neuroscientific paradigm of general anesthesia and related states of unconsciousness. Neurosci. Biobehav. Rev. 37, 2751–2759 (2013).

76. R. Baker et al., Altered activity in the central medial thalamus precedes changes in the neocortex during transitions into both sleep and propofol anesthesia. J. Neurosci. 34, 13326–13335 (2014).

77. B. B. Theyel, D. A. Llano, S. M. Sherman, The corticothalamocortical circuit drives higher-order cortex in the mouse. Nat. Neurosci. 13, 84–88 (2010).

78. C. D. Gilbert, M. Sigman, Brain states: Top-down influences in sensory processing. Neuron 54, 677–696 (2007).

79. W. A. Phillips, M. E. Larkum, C. W. Harley, S. M. Silverstein, The effects of arousal on apical amplification and conscious state. Neurosci. Conscious. 2016, niw015 (2016).

80. G. Tononi, M. Boly, M. Massimini, C. Koch, Integrated information theory: From consciousness to its physical substrate. Nat. Rev. Neurosci. 17, 450–461 (2016).

81. S. Dehaene, J.-P. Changeux, Experimental and theoretical approaches to conscious processing. Neuron 70, 200–227 (2011).

82. B. Marsh, M. White, N. Morton, G. N. Kenny, Pharmacokinetic model driven infusion of propofol in children. Br. J. Anaesth. 67, 41–48 (1991).

NEUROSCIENCE

83. A. R. Absalom, V. Mani, T. De Smet, M. M. R. F. Struys, Pharmacokinetic models for propofol–Defining and illuminating the devil in the detail. *Br. J. Anaesth.* **103**, 26–37 (2009).

84. S. Cascone, G. Lamberti, G. Titomanlio, O. Piazza, Pharmacokinetics of Remifentanil: A three-compartment modeling approach. *Transl. Med. UniSa* **7**, 18–22 (2013).

85. ALARIS, Arsena PK syringe pump manual (Alaris Medical Systems, 2004).

86. I. Fried *et al.*, Cerebral microdialysis combined with single-neuron and electroencephalographic recording in neurosurgical patients. Technical note. *J. Neurosurg.* **91**, 697–705 (1999).

87. J. Talairach, P. Tournoux, *Co-Planar Stereotaxic Atlas of the Human Brain: 3-Dimensional Proportional System: An Approach to Cerebral Imaging* (Thieme Medical Publishers, 1988).

88. D. A. Chernik *et al.*, Validity and reliability of the observer's assessment of alertness/sedation scale: Study with intravenous midazolam. *J. Clin. Psychopharmacol.* **10**, 244–251 (1990).

89. R. Munglani, J. Andrade, D. J. Sapsford, A. Baddeley, J. G. Jones, A measure of consciousness and memory during isoflurane administration: The coherent frequency. *Br. J. Anaesth.* **71**, 633–641 (1993).

90. S. Makeig, S. Debener, J. Onton, A. Delorme, Mining event-related brain dynamics. *Trends Cogn. Sci.* **8**, 204–210 (2004).

91. C. Tallon-Baudry, O. Bertrand, C. Delpuech, J. Pernier, Stimulus specificity of phase-locked and non-phase-locked 40 Hz visual responses in human. *J. Neurosci.* **16**, 4240–4249 (1996).

92. J. H. Zar, "Equation 27.4" in *Biostatistical Analysis* (Prentice Hall, ed. 5, 2010), p. 625.

93. E. B. Issa, X. Wang, Sensory responses during sleep in primate primary and secondary auditory cortex. *J. Neurosci.* **28**, 14467–14480 (2008).

94. R. Q. Quiroga, Z. Nadasdy, Y. Ben-Shaul, Unsupervised spike detection and sorting with wavelets and superparamagnetic clustering. *Neural Comput.* **16**, 1661–1687 (2004).

95. Y. Nir *et al.*, Selective neuronal lapses precede human cognitive lapses following sleep deprivation. *Nat. Med.* **23**, 1474–1480 (2017).

www.manaraa.com